International Journal of Multimedia and Ubiquitous Engineering
Vol.9, No.5 (2014), pp.155-168
http://dx.doi.org/10.14257/ijmue.2014.9.5.15

Surface Reconstruction from Gradient Fields Using Box-Spline Kernel

Guodong Wang[1, 2], Jingbao Yang[2], Yue Cheng[2*]

[1]*School of Computer Science, Northwestern Polytechnical University, Xi'an, China*
[2]*AVIC Computing Technique Research Institute, Xi'an, China*
chengyue198552@gmail.com[*]

Abstract

Surface reconstruction from gradient fields is of wide application in computer vision fields. Traditional methods usually enforce surface integrability in discrete domain, while current kernel approach suffers the problems of parameter choice. In this paper, we propose a novel method, i.e. kernel gradient regression, to reliably reconstruct surfaces. The box-spline kernel, instead of the common Gaussian kernel, is deployed in surface reconstruction due to its compact support and parameter robustness. To our knowledge, this is the first time to prove the special box-spline function as a new kind of positive definite spline kernel. The target surface is recovered under least-squares sense from the gradient fields, by converting the reconstruction problem to its kernel representation. Experimental results show that our proposed method outperform available approaches in preserving sharp edges and fine details, without prior knowledge of depth discontinuity.

Keywords: *Kernel, Box-spline, Reconstruction*

1. Introduction

Three-dimensional surface reconstruction is an important branch of Computer Vision. It plays an important role in the quality control of products, industrial measurement, medical diagnosis, digital preservation of relic, scene evidence, digital entertainment and virtual reality. In some application areas, local features of measured object can not be well reconstructed based on the direct geometric measurement method which makes the details of reconstructed surface quality greatly degraded, and often can not meet the requirements. On the other hand, surface reconstruction from gradient fields scheme can keep local details of measured objects well. It is quite satisfactory for computer vision applications and greatly complement geometric measurement based methods. Thus gradient fields surface reconstruction has received wide attention in the research field, and has become a key post-processing step in shape from shading [1, 2], photometric stereo [3], and shape from texture [4, 5].

Typically, in the gradient reconstruction non-integrable gradient fields are produced in the first step, thus further processing is necessary to obtain the final surfaces. Traditional methods project the non-integrable gradient fields to the integrable gradient fields, such as Fourier bases [6], orthogonal wavelets bases [7], or redundant non-orthogonal shapelets basis functions [8]. Other methods use the zero-curl assumption to produce integrable gradient fields [9-11]. Alternatively, Harker and O'Leary [12] use discrete least squares to reconstruct surface from gradient fields ignoring the integrability of objective surface.

ISSN: 1975-0080 IJMUE

Over the last ten years kernel methods [13, 14] attracted intensive attention in the pattern recognition and machine learning literature. These methods formulate learning and estimation problems in a reproducing kernel Hilbert space (RKHS) [15]. The familiar problems, including regression, classification, and principal component analysis, can be resolved using kernel techniques [16, 17]. By applying kernel trick [15], the nonlinear data can be mapped to RKHS, and the high-dimensional property of the feature space makes the algorithm linear and easy to handle. The convenient kernel method provides the opportunity to other important applications, for example, surface reconstruction from gradient fields. Most recently, Ng *et al.* [18] applied kernel approach to reconstruct surface without enforcing integrability. This method treats the reconstruction problem as kernel regression, which approximates the underlying surface by kernel density estimation. It calculates the dual form of regression parameters by minimizing the dot-product between kernel represented gradients and observed normals. This method could not maintain sharp edges, and requires prior knowledge of depth discontinuity for certain surfaces.

Like most kernel approaches, Ng *et al.* [18] also used the common Gaussian kernel, which is of infinite support, in their kernel reconstruction approach. Theoretically, the calculation of all dot-products in neighboring sites can result in a dense Gram matrix [15], which is computational very expensive. Practically, the truncated Gaussian function can be employed instead. However, it is always difficult to determine the appropriate parameter values (variance and cut-off radius) in surface reconstruction.

In this paper, we propose a kernel method to reconstruct surface from gradient fields. We kernelize the gradient regression problem such that surface reconstruction can be resolved by least squares in the dual space. In addition, we prove that a special box-spline function [19] can be used as positive definite kernel. As box-spline kernel is compactly supported, the reconstruction accuracy can be improved and the computation is quite efficient. The proposed kernel method are evaluated by both synthetic gradient data and simulated photometric stereo.

The rest of the paper is organized as follows. Section 2 presents the background and related work. Section 3 outlines our proposed gradient surface reconstruction method using kernel. Section 4 proves that a special box-spline function is a new kind of kernel. Section 5 presents the results. Finally, conclusion and future work are discussed.

2. Related Work

In this section, we first review the relevant work on traditional surface reconstruction methods, and then introduce the background of box-spline functions.

2.1. Surface Reconstruction

The efficient solution to surface reconstruction problem is projecting the non-integrable gradients to the frequency domain [6] or wavelet domain [7, 20], and then surface is integrated in this fields. As an extension, Kovesi [8] used redundant non-orthogonal shapelets as basis functions, which made the reconstruction more robust. This method also used the slant and tilt data as input rather than the gradient ones to avoid over-smooth. It shared the same idea that the differentiation in frequency domain will become linear, resulting in an easier and more efficient solution. Among these projecting methods, Simchony *el al.*'s [21] is the most classical one. In their paper two direct analytical methods were proposed to solve the reconstruction problem. In order to translate the original scene depth to frequency domain, they used discrete sine transform (DST) for Dirichlet boundary conditions and discrete cosine transform (DCT) for Neumann boundary conditions [22]. It was reported that the precision and

robustness of these methods were superior to other methods [23, 24]. In most situations, since the objective surface is smooth enough to fit Neumann boundary conditions, so DCT transform for gradient fields is quite suitable for surface reconstruction. But when large changes like sharp edges appear on the surface, DCT fails to give satisfactory results. Thus more robust method is demanded to solve universal problem. Following Simchony *et al.*'s work, Agrawal *et al.* [9-11] presented a framework for a series of integral enforcing methods. They modified the objective function leading to slight changes in corresponding Euler-Lagrange equation. The yielded binary weighted Poisson equation was used in alpha-surface method and continuous weighted Poisson equation was used in M-estimators method. These methods iteratively updated the weights according to local information after obtaining the initial result using the DCT method [21].

On the other hand, Harker and O'Leary [12] proposed a direct and non-iterative reconstructing method in spatial domain. This method used the finite difference form of local gradient fields to construct an overall objective function. The finite difference operation is only related to several neighbor pixels, thus the overall difference matrix is quite sparse which makes the large scale reconstruction of reliable surface practical. While in this method only limited local information of the objective surface had been involved into calculation, so it failed to reconstruct a satisfactory surface when the noise in gradient fields was really severe. Noticeably, this method ignored the integrability of objective surface which was different from the above-mentioned methods.

Although all the methods mentioned above solved the surface reconstruction problem in frequency domain or in spatial domain, intrinsically they need complete gradient data input. In addition, these methods cannot control the smoothness level of the target surface. Ng *et al.* [18] proposed to solve the reconstruction problem by using a kernel approach. By constructing the kernel form of the surface function, the reconstruction problem was transformed to linear regression in the kernel feature space. The algorithm was also applicable to sparse input, thanks to the regulation term in its solution. However, this method did not consider the sharp changes on the target surface and would fail to reconstruct surface when the surface has sharp edges.

2.2. Box-spline

Box-splines [19] are nontrivial generalization of one-dimensional uniform B-splines to higher dimensions. It consists of piecewise polynomials and has global continuity and compact support. Unlike tensor form B-spline, whose support is a rectangle, box-splines have more flexible supports which include B-spline's as a special case. Box-spline is superior to B-spline also in the Fourier domain. The frequency of B-spline, due to its tensor product inherence, decays faster along the diagonal directions than the grid directions. Consequently, according to Shannon's sampling theory, box-spline is more adequate than B-spline in surface reconstruction.

Box-spline plays an important role in the field of multi-dimensional function approximation, due to its elegant properties. Recently, box-spline was widely use for volume reconstruction and rendering, where the volume data are non-Cartesian sampled [25-27]. Entezari and Möller [28] extended the well-known Zwart-Powell box-spline in 2-D to a 7-direction box-spline in 3-D and used it to reconstruct Cartesian lattice volume data.

For a long time, there lacks efficient algorithms to evaluate box-splines. Recently, Kim and Peter [29] proposed an evaluation algorithm based on Beziér form, and proved

that their algorithm is efficient and accurate. We also employed this algorithm in our work and found that it is indeed adequate for practical use.

In previous work [25, 26, 28], box-splines were directly used as interpolation approximations for volume data reconstruction, and their performance was evaluated in Fourier domain. To our knowledge, we are the first one to construct a positive definite box-spline kernel and validate its performance in the sense of RKHS. Differing from other kernel functions, box-spline kernel function is compact supported, which make it easier to choose function parameters and give precise reconstruction results. The details of box-spline kernel will be given in the following section.

3. Surface Reconstruction by Kernel Method

In this section, we introduce the kernel regression method of surface reconstruction. Because of the analytic form of the regression function, the surface gradients could also be represented in similar kernel form preserving the same regression parameters. Thus the surface parameters are recovered under least-squares sense from the kernelized gradient fields.

3.1. Surface Reconstruction

Consider a linear regression problem [16]

$$z = f(\mathbf{x}) = <\mathbf{w}, \mathbf{x}> = \sum_{i=1}^{n} w_i x_i, \tag{1}$$

which fits the training set $S = \{(\mathbf{x}_1; z_1), \cdots, (\mathbf{x}_l; z_l)\}$, where $\mathbf{x} \in \square^n$ has the corresponding label z. Here, we use the notation $\mathbf{x} = (x_1, x_2, \cdots, x_n)^{\mathrm{T}}$ for the n-dimensional input, and $\mathbf{w}$ for the n-dimensional regression parameter.

Equation (1) can be written in its dual representation

$$f(\mathbf{x}) = \langle \mathbf{X}\boldsymbol{\alpha}, \mathbf{x} \rangle = \sum_{i=1}^{l} \alpha_i \langle \mathbf{x}_i, \mathbf{x} \rangle, \tag{2}$$

where $\mathbf{X} = (\mathbf{x}_1, \mathbf{x}_2, \cdots, \mathbf{x}_l)^{\mathrm{T}}$. By applying kernel trick, we get the kernel form of the regression equation as

$$f(\mathbf{x}) = \sum_{i=1}^{l} \alpha_i k(\mathbf{x}_i, \mathbf{x}), \tag{3}$$

which maps the low-dimensional data to high-dimensional kernel space. It is note that [16], as a kernel function, $k(\mathbf{x}_i, \mathbf{x})$ must obey the reproducing property

$$k(\mathbf{x}_i, \mathbf{x}) = <\phi(\mathbf{x}_i), \phi(\mathbf{x})>, \tag{4}$$

where $\phi(\mathrm{x})$ denotes the nonlinear feature space mapping.

In our surface reconstruction problem, $\mathbf{x} = (u, v)^{\mathrm{T}}$ is the surface site and $z = f(\mathbf{x})$ is its corresponding depth, and $\mathbf{x}_i$ is the neighboring site of $\mathbf{x}$. Let $\mathbf{z} = (f(\mathbf{x}_1), f(\mathbf{x}_2), \cdots, f(\mathbf{x}_l))^{\mathrm{T}}$ and substitute the observed data in the kernel representation, we have

$$\begin{aligned} \mathbf{z} &= \begin{pmatrix} k(\mathbf{x}_1,\mathbf{x}_1) & \cdots & k(\mathbf{x}_1,\mathbf{x}_l) \\ k(\mathbf{x}_2,\mathbf{x}_1) & \cdots & k(\mathbf{x}_2,\mathbf{x}_l) \\ \vdots & \vdots & \vdots \\ k(\mathbf{x}_l,\mathbf{x}_1) & \cdots & k(\mathbf{x}_l,\mathbf{x}_l) \end{pmatrix} \begin{pmatrix} \alpha_1 \\ \alpha_2 \\ \vdots \\ \alpha_l \end{pmatrix} \\ &= \mathbf{G}\boldsymbol{\alpha}, \end{aligned} \tag{5}$$

where $\mathbf{G}$ is the Gram matrix of the kernel function. By this manner, the nonlinear regression problem becomes linear in the dual space. It is clear from Equation (5) that, the surface can be reconstructed when we know the regression parameter $\boldsymbol{\alpha}$.

As the gradient fields, not depths, are available in surface reconstruction problem, we could compute $\boldsymbol{\alpha}$ from the derivation of Equation (3). Based on this consideration, we present the kernel gradient regression method in the following sections.

3.2. Kernel Gradient Regression

According to the analytic form described in Equation (3), the surface will be differentiable if an appropriate kernel function is chosen. We can obtain the first order derivative of Equation (3) as

$$\begin{aligned} f_a(\mathbf{x}) &= \frac{\partial\left\{\sum_{i=1}^{l}\alpha_i k(\mathbf{x}_i,\mathbf{x})\right\}}{\partial a} \\ &= \sum_{i=1}^{l}\alpha_i \frac{\partial k(\mathbf{x}_i,\mathbf{x})}{\partial a} \\ &= \sum_{i=1}^{l}\alpha_i k_a(\mathbf{x}_i,\mathbf{x}), \end{aligned} \tag{6}$$

where $a \in (u,v)$. Let $\mathbf{z}_a = (f_a(\mathbf{x}_1), f_a(\mathbf{x}_2), \cdots, f_a(\mathbf{x}_l))^{\mathrm{T}}$, it can be written as

$$\begin{aligned} \mathbf{z}_a &= \begin{pmatrix} k_a(\mathbf{x}_1,\mathbf{x}_1) & \cdots & k_a(\mathbf{x}_1,\mathbf{x}_l) \\ k_a(\mathbf{x}_2,\mathbf{x}_1) & \cdots & k_a(\mathbf{x}_2,\mathbf{x}_l) \\ \vdots & \vdots & \vdots \\ k_a(\mathbf{x}_l,\mathbf{x}_1) & \cdots & k_a(\mathbf{x}_l,\mathbf{x}_l) \end{pmatrix} \begin{pmatrix} \alpha_1 \\ \alpha_2 \\ \vdots \\ \alpha_l \end{pmatrix} \\ &= \mathrm{G}_a\boldsymbol{\alpha}. \end{aligned} \tag{7}$$

Similarly, by applying 2-order differentiation, we also get the Laplacian of the surface as

$$\begin{aligned} f_{\mathrm{L}}(\mathbf{x}) &= \frac{\partial^2 f(\mathbf{x})}{\partial u^2} + \frac{\partial^2 f(\mathbf{x})}{\partial v^2} \\ &= \sum_{i=1}^{l}\alpha_i\left(\frac{\partial^2 k(\mathbf{x}_i,\mathbf{x})}{\partial u^2} + \frac{\partial^2 k(\mathbf{x}_i,\mathbf{x})}{\partial v^2}\right) \\ &= \sum_{i=1}^{l}\alpha_i k_{\mathrm{L}}(\mathbf{x}_i,\mathbf{x}). \end{aligned} \tag{8}$$

Let $\mathbf{z}_L = (f_L(\mathbf{x}_1); f_L(\mathbf{x}_2), \cdots, f_L(\mathbf{x}_l))^T$, Equation (8) can be written in the matrix notation as

$$\begin{aligned} \mathbf{z}_L &= \begin{pmatrix} k_L(\mathbf{x}_1,\mathbf{x}_1) & \cdots & k_L(\mathbf{x}_1,\mathbf{x}_l) \\ k_L(\mathbf{x}_2,\mathbf{x}_1) & \cdots & k_L(\mathbf{x}_2,\mathbf{x}_l) \\ \vdots & \vdots & \vdots \\ k_L(\mathbf{x}_l,\mathbf{x}_1) & \cdots & k_L(\mathbf{x}_l,\mathbf{x}_l) \end{pmatrix} \begin{pmatrix} \alpha_1 \\ \alpha_2 \\ \vdots \\ \alpha_l \end{pmatrix} \\ &= \mathbf{G}_L \boldsymbol{\alpha}, \end{aligned} \tag{9}$$

where $\mathbf{G}_L$ is referred as Laplacian Gram matrix in this work. Equation (9) is actually the Poisson equation in the kernel representation.

Therefore we can obtain the parameter $\boldsymbol{\alpha}$ from the matrix form equation (7). By further adding a regularization term, which can be the local Laplacian, to control the smoothness of the target surface, we write the objective function in quadric form as

$$E(\boldsymbol{\alpha}) = \| \mathbf{z}_a - \mathbf{G}_a \boldsymbol{\alpha} \|^2 + \lambda \| \mathbf{z}_L \|^2, \tag{10}$$

where λ is the weight of the regularization term.

The kernel regression parameter $\boldsymbol{\alpha}$ can be calculated by setting the first order derivative of $E(\boldsymbol{\alpha})$ to zero. Then the target surface can be reconstructed as

$$\mathbf{z} = \mathbf{G}\boldsymbol{\alpha} = \mathbf{G}\left(\mathbf{G}_a^T \mathbf{G}_a + \lambda \mathbf{G}_L^T \mathbf{G}_L \right)^{-1} \mathbf{z}_a^T \mathbf{G}_a. \tag{11}$$

4. Box-spline Kernel

Box-splines offer a mathematically elegant framework for constructing a class of elements with flexible shape and support, and have been successfully applied in volume data reconstruction and rendering [25, 26]. In this section, we first briefly introduce box-spline, then prove that a specific box-spline function can serve as kernels, and finally validate its superiority in surface reconstruction over the common Gaussian and B-spline kernels.

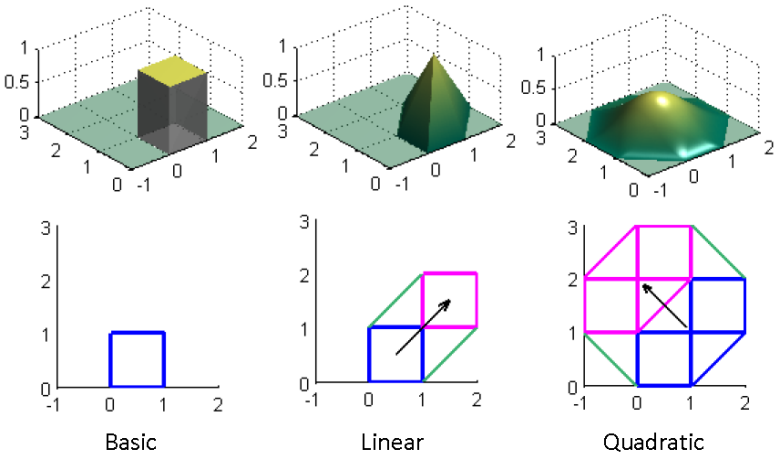

Figure 1. Illustration of Box-Splines Generation. The Top Row shows the Shape of the Basic, Linear, and Quadratic Box-Splines and the Bottom Row Shows their Corresponding Support Regions. Higher-order Box-Splines are generated from the Lower-Order Ones by "Smearing" Along the Specified Directions

4.1. Definition and Properties

A box-spline is specified by n vectors in $\mathbb{R}^s$ where $n > s$, and is denoted by $\Xi_{s\times n} = (\xi_1, \cdots, \xi_n)$. For the surface reconstruction in this work $s = 2$. The simplest box-spline is constructed by n = s vectors, which is the characteristic function of its support

$$M_{\Xi}(x) = \begin{cases} \dfrac{1}{|\det \Xi|}, & x \in \Xi[0,1)^n \\ 0, & otherwise \end{cases}, \tag{12}$$

where $\Xi[0,1)^n$ denotes the support and $|\det \Xi|$ is its corresponding area. In the case of $n > s$, box-splines are defined recursively

$$M_{[\Xi,\xi]} = \int_0^1 M_{\Xi}(\mathbf{x} - t\xi)\, dt, \tag{13}$$

which means that $M_{[\Xi,\xi]}$ is obtained by "smearing" $M_{\Xi}(x)$ along the direction of vector ξ. Then starting from the basic box-spline specified by Equation (12), higher order ones can be generated recursively by Equation (13). Figure 1 illustrates this intuitive generation procedure.

Usually, box-splines defined by the above formula do not center at the origin, see Figure 1. For convenience, we translate their centers to the origin and still denote them by $M_{\Xi}(x)$.

The Fourier transformation of the centralized box-spline is given by:

$$\hat{M}_{\Xi}(\boldsymbol{\omega}) = \prod_{\xi\in\Xi} \left(\operatorname{sinc}\left(\boldsymbol{\omega}^T \xi\right)\right), \tag{14}$$

where $\boldsymbol{\omega} = (\omega_1, \omega_2, \cdots, \omega_n)^T$ is the vector in Fourier domain and $\operatorname{sinc}(x) = \sin(x/2)/(x/2)$. A comprehensive introduction to box-splines can be found in [19].

4.2. Proof of Kernel

The dot-product kernel in Equation (4) coincides with the class of positive definite kernel. Hofmann *et al.* [14] state the following theorem for positive definite function.

Theorem 1 *A continuous function h on $\mathbb{R}^d$ is positive definite if and only if there exists a finite nonnegative Borel measure μ on $\mathbb{R}^d$ such that*

$$h(x) = \int_{\mathbb{R}^d} e^{-i\langle \mathbf{x}, \boldsymbol{\omega}\rangle} d\mu(\boldsymbol{\omega}) \tag{15}$$

Informally, this means that h is positive definite if and only if its Fourier transform is nonnegative.

We start with the famous Zwart-Powell (ZP) [28] box-spline. In the 2-D form, ZP box-spline is specified by

$$\Xi_{ZP} = \begin{pmatrix} 1 & 0 & 1 & -1 \\ 0 & 1 & 1 & 1 \end{pmatrix}. \tag{16}$$

As this box-spline does not make a kernel, we construct a new one by specifying $\Xi = (\Xi_{ZP}, \Xi_{ZP})$, whose Fourier transform is

$$\hat{M}_{\Xi} = \mathrm{sinc}^2(\omega_u)\mathrm{sinc}^2(\omega_v)\mathrm{sinc}^2(\omega_u + \omega_v)\mathrm{sinc}^2(-\omega_u + \omega_v), \tag{17}$$

where ω_u and ω_v are the frequencies along the u and v directions, respectively.As $\hat{M}_{\Xi}$ is nonnegative, M_{Ξ} is positive definite according to Theorem 1, and hence can serve as a positive definite kernel, i.e.

$$k(\mathbf{x}, \mathbf{x}_i) = M_{\Xi}(\mathbf{x} - \mathbf{x}_i). \tag{18}$$

4.3. Kernel Comparison

In this section, we discuss the support properties of the box-spline, Gaussian, and B-spline kernels, and compare the reconstruction accuracy of these kernels.

The commonly used Gaussian kernel is of the form

$$k(\mathbf{x}, \mathbf{x}_i) = \exp\left(\frac{-\|\mathbf{x} - \mathbf{x}_i\|^2}{2\sigma^2}\right), \tag{19}$$

which is a radius basis function (RBF) kernel. Its shape is determined by the variance parameter σ.

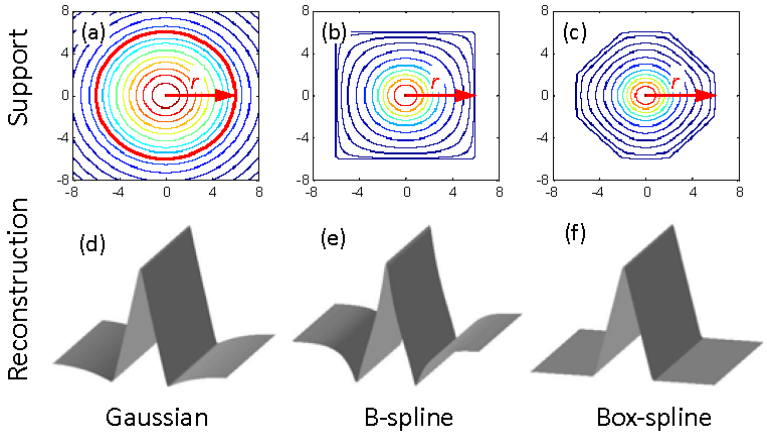

Figure 2. Reconstructed Ridge Surface using Different Kernel Functions. Top: The Supports of Gaussian, B-spline, and box-spline Functions. Bottom: Reconstructed Ridge Surfaces from its Gradients

As Gaussian kernel is of infinite support (see Figure 2(a)), theoretically its Gram matrices $\mathbf{G}_a$ and $\mathbf{G}_L$ will be full matrices which needs expensive computation. For truncated Gaussian kernel in practice, it is still difficult to determine the suitable cut-off radius r and variance σ.

As shown in Figure 2(b), B-spline kernel function is compactly supported and its support is square at the edge. In addition, the B-spline function is anisotropic with respect to the center, thus it's not a RBF kernel. Figure 2(c) illustrates that the support of box-spline kernel is compact, which makes the Gram matrices quite sparse. As the

octagon support is nearly isotropic, box-spline kernel can be approximately regarded as a RBF kernel.

In the following, we compare the performances of the three kernels in surface reconstruction. For the box-spline and B-spline kernels, it is natural to choose the support boundary as their radius r. For the Gaussian kernel, we need to determine both its cut-off radius r and variance σ. For convenience, we relate r and σ by a factor n such that $\sigma = r/n$.

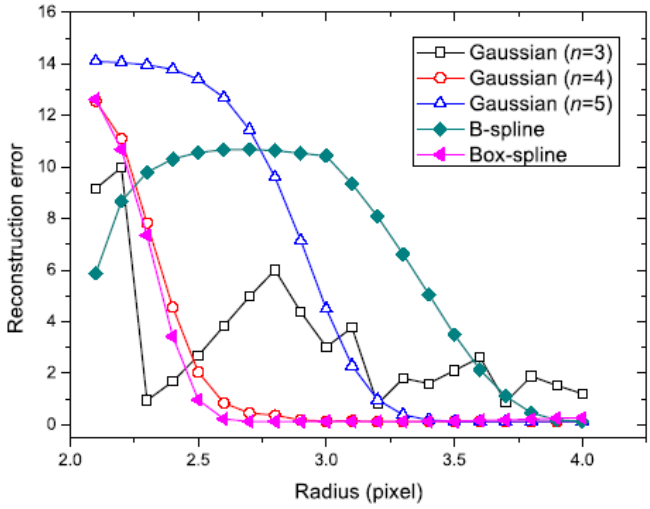

Figure 3. Reconstruction Errors of Ridge Surface with Respect to Support Radius for Three Kernel Functions

We constructed a Ridge surface with two symmetric narrow elevations and a float floor, and used the proposed kernel gradient regression method to reconstruct the Ridge surface from its gradient fields. Figure 3 shows the reconstruction root-mean-square (RMS) errors of the box-spline, B-spline, and Gaussian ($n = 3,4,5$) kernels, with respect to different radius values. For the box-spline kernel, the reconstruction error decreases quickly and become stable when $r \geq 2.6$. For the Gaussian kernel, the reconstruction error is sensitive to both cut-off radius and variance. Its reconstruction is quite instable when $n = 3$, and close to that of box-spline kernel in case of $n = 4$. The reconstruction error of the B-spline kernel is also relatively large. Overall, the surface reconstruction by box-spline kernel is quite accurate, and is robust to the radius parameter. Figure 2 shows the reconstructed Ridge surfaces under the same radius $r = 3.0$ (for Gaussian kernel, $\sigma = 3.0$). We note that, for other surfaces, the error distributions of Gaussian become different, which prevents the use of fixed parameters. In the following section, we use box-spline kernel in the proposed method without specific notation.

5. Experimental Results

In the experiment, we evaluate the proposed method on both synthetic gradient data and in simulated photometric stereo, in comparison with the DCT, alpha-surface [10], M-estimation [10] and Frankot-Chellappa method [6].

5.1. Synthetic Data

The reconstruction results on noise-free Vase data are shown in Figure 4. Overall, Frankot-Chellappa method totally fails with a large deforming after reconstruction. A better shape is obtained by Alpha surface method, but there is an obvious bias at the left-side of the vase surface. The reconstructed surfaces by the DCT and M-estimator methods seem good, but oscillations occur at sharp edges (see enlarged parts). This is because the gradient data is obtained approximately using finite difference scheme from local surface. In comparison, the proposed kernel method produce satisfactory reconstructions. The reconstructed surface not only well maintains the overall shape of the vase but also keep the smoother fine details.

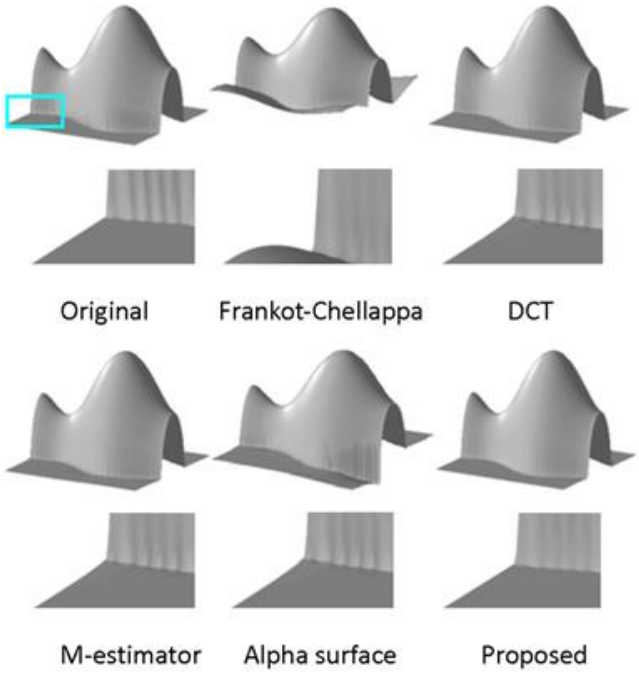

Figure 4. Reconstructed Vase surfaces without Noise. The Enlarged Parts show Detail Comparison

Next, we make the gradient data of a Ramp surface and added Gaussian noise with $\sigma = 5\%$ of its maximum gradient. The reconstructed surfaces are shown in Figure 5. The reconstruction by the alpha-surface is heavily affected by noise, the vibration is throughout the whole surface. For the Frankot-Chellappa, DCT and M-estimator methods, although the noise is well suppressed, the reconstructed pyramid base are obviously distorted (the error parts are pointed by the arrows). In comparison, the proposed method successfully reconstruct this noise-corrupted surface. The noise is better reduced and the smooth pyramid base is also well maintained.

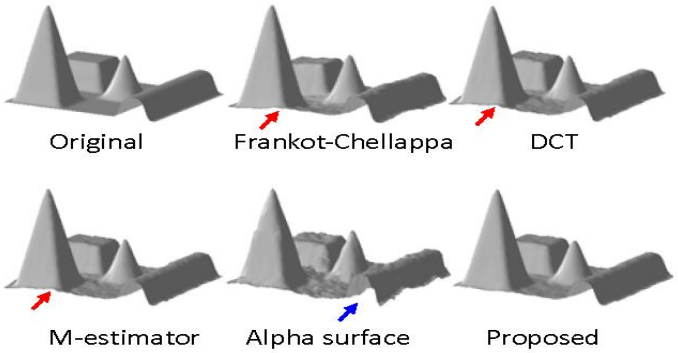

Figure 5. Reconstructed Ramp Surfaces with Additive Gaussian Noises ($\sigma = 5\%$) of the Maximum Gradient in the Gradient Fields. The Arrows Indicate the Surface Parts that are not Appropriately Reconstructed

Table 1 gives the RMS errors of different reconstruction methods for the Vase and Ramp surfaces. It is verified that the proposed kernel method produces the best reconstruction accuracy in both noisy and noise-free data.

Table 1. Root-mean-square Errors of Different Reconstruction Methods on Noisy and noise-free Gradient Data

Method	**w/o noise**		**with noise**	
	Vase	***Ramp***	***Vase***	***Ramp***
Frankot-Chellappa [6]	2.38	0.30	2.39	0.30
DCT [10]	0.47	0.33	0.56	0.35
Alpha surface[10]	1.80	0.72	3.45	0.82
M-estimator [10]	0.47	0.33	0.57	0.35
Proposed	**0.19**	**0.09**	**0.33**	**0.13**

5.2. Simulated Photometric Stereo

We generate eight Mozart images under different lighting directions according to the Lambertian model, and add Gaussian noise (with $\sigma = 10\%$ of the maximum intensity) to simulate the actual imaging procedure. Three of these images are shown in Figure 6. We then employ the traditional photometric stereo [3] algorithm to estimate the surface normals, based on which gradient fields were obtained.

Figure 6. Three Simulated Mozart Images (Out Of Eight Ones) under Different Lighting Directions, Added with Gaussian Random Noises($\sigma = 10\%$) of the Maximum Intensity

Figure 7 shows the reconstructed Mozart surfaces by different methods. Frankot-Chellappa and DCT methods produce oscillating results on the large gradient regions. Alpha surface and M-estimator methods suppress this oscillation but the appearances are noisy. In contrast, proposed method maintains large curvatures in the sharp change areas, and preserve fine details at the same time.

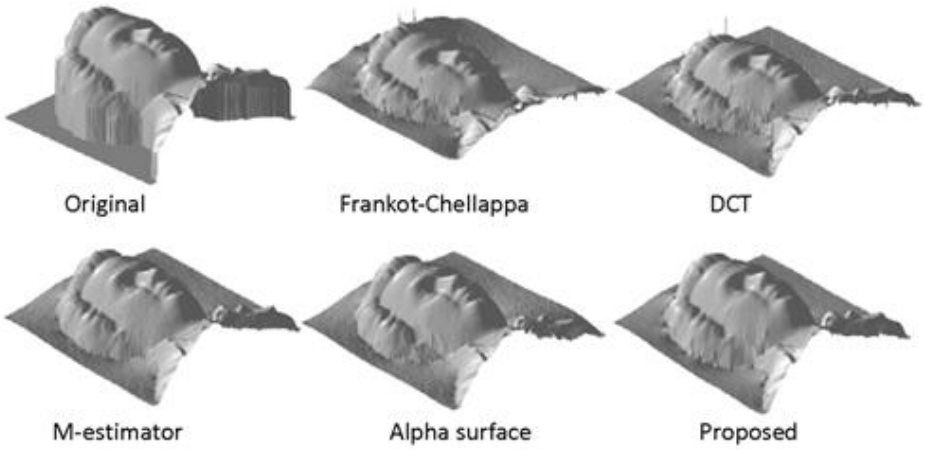

Figure 7. Reconstructed Mozart Surfaces in Simulated Photometric Stereo by Different Methods

6. Conclusions

We have presented the kernel gradient regression method to reconstruct surfaces from gradient fields. In addition, we construct a specific box-spline kernel that is superior to the common Gaussian and B-spline kernels. To our knowledge, we are the first one to propose this new kind of positive definite kernel function and prove it in the previous section. Experimental results validate that the proposed kernel method outperform other reconstruction methods on both synthetic gradient data and in simulated photometric stereo. Proposed method is of practical application in related computer vision fields including photometric stereo, shape from shading, etc. On the other hand the disadvantage of proposed method is time-consuming, in the future the acceleratory scheme should be carefully designed, for example, parallel computing based on GPU platform. The radius of kernel function is quite related to noise level, if we estimate the gradient noise level firstly, then the only parameter of box-spline function could be fixed, which make the reconstruction more convenient and precise. We can expect that these improvement will help the box-spline kernel reconstruction scheme become a more widely used method in surface reconstruction field.

References

[1] B. K. P. Horn, "Shape from shading: A method for obtaining the shape of a smooth opaque object from one view", M.I.T. Technical Report **(1970)**.
[2] R. Zhang, P. S. Tsai, J. E. Cryer and M. Shah, "Shape from shading: a survey", IEEE Transactions on Pattern Analysis and Machine Intelligence, vol. 21, no. 8, **(1999)**, pp. 690-706.
[3] R. J. Woodham, "Photometric method for determining surface orientation from multiple images", Optical Engineering, vol. 19, no. 1, **(1980)**, pp. 139-144.
[4] M. Clerc and S. Mallat, "The texture gradient equation for recovering shape from texture", IEEE Transactions on Pattern Analysis and Machine Intelligence, vol. 24, no. 4, **(2002)**, pp. 536-549.
[5] D. A. Forsyth, "Shape from texture and integrability", Proceedings of IEEE International Conference on Computer Vision (ICCV), **(2001)**, pp. 447-452.

[6] R. T. Frankot and R. Chellappa, "A method for enforcing integrability in shape from shading algorithms", IEEE Transactions on Pattern Analysis and Machine Intelligence, vol. 10, no. 4, **(1988)**, pp. 439-451.
[7] B. Karacali and W. Snyder, "Noise reduction in surface reconstruction from a given gradient field", International Journal of Computer Vision, vol. 60, no. 1, **(2004)**, pp. 25-44.
[8] P. Kovesi, "Shapelets correlated with surface normals produce surfaces", Proceedings of IEEE International Conference on Computer Vision (ICCV), **(2005)**, pp. 994-1001.
[9] A. Agrawal, R. Chellappa, and R. Raskar, "An algebraic approach to surface reconstruction from gradient fields", Proceedings of IEEE International Conference on Computer Vision (ICCV), **(2005)**, pp. 174-181.
[10] A. Agrawal, R. Raskar, and R. Chellappa, "What is the range of surface reconstructions from a gradient field?", Proceedings of European Conference on Computer Vision (ECCV), **(2006)**, pp. 578-591.
[11] D. Reddy, A. Agrawal, and R. Chellappa, "Enforcing integrability by error correction using ℓ1-minimization", Proceedings of IEEE Conference on Computer Vision and Pattern Recognition (CVPR), **(2009)**, pp. 2350-2357.
[12] M. Harker and P. O'Leary," Least squares surface reconstruction from measured gradient fields", Proceedings of IEEE Conference on Computer Vision and Pattern Recognition (CVPR), **(2008)**, pp. 1-7.
[13] T. Hofmann, B. Schölkopf and A. J. Smola, "A review of kernel methods in machine learning", Mac-Planck-Institute Technical Report 156, **(2006)**.
[14] T. Hofmann, B. Schölkopf, and A. J. Smola, "Kernel methods in machine learning", The Annals of Statistics, **(2008)**, pp. 1171-1220.
[15] J. Shawe-Taylor and N. Cristianini, "Kernel Methods for Pattern Analysis", Cambridge University Press, **(2004)**.
[16] C. M. Bishop, "Pattern Recognition and Machine Learning", Springer, **(2006)**.
[17] B. Scölkopf and A. J. Smola, "Learning with Kernels". The MIT Press, **(2002)**.
[18] H. S. Ng, T. P. Wu, and C. K. Tang. "Surface-from-gradients without discrete integrability enforcement: a gaussian kernel approach", IEEE Transactions on Pattern Analysis and Machine Intelligence, vol. 32, no. 11, **(2009)**, pp. 2085-2099.
[19] C. de. Boor, K. Höllig, and S. D. Riemenschneider, "Box Splines", Springer, **(1993)**.
[20] B. Karacali and W. Snyder. "Partial integrability in surface reconstruction from a given gradient field", In IEEE International Conference on Image Processing, vol. 2, **(2002)**, pp. II-525.
[21] T. Simchony, R. Chellappa, and M. Shao, "Direct analytical methods for solving poisson equations in computer vision problems", IEEE Transactions on Pattern Analysis and Machine Intelligence, vol. 12, no. 5, **(2002)**, pp. 435-446.
[22] A. Cheng and D. T. Cheng, "Heritage and early history of the boundary element method", Engineering Analysis with Boundary Elements, vol. 29, no. 3, **(2005)**, pp. 268-302.
[23] B. L. Buzbee, G. H. Golub and C. W. Nielson, "On direct methods for solving poisson's equations". SIAM Journal on Numerical analysis, vol. 7, no. 4, **(1970)**, pp. 627-656.
[24] R. W. Hockney, "A fast direct solution of poisson's equation using fourier analysis". Journal of the ACM, vol. 12, no. 1, **(1965)**, pp. 95-113.
[25] A. Entezari, V. D. Ville and T. Möller, "Practical box splines for reconstruction on the body centered cubic lattice". IEEE Transactions on Visualization and Computer Graphics, vol. 14, no. 2, **(2007)**, pp. 313-328.
[26] B. Finkbeiner, A. Entezari, D. V. D. Ville and T. Möller, "Efficient volume rendering on the body centered cubic lattice using box splines", Computers & Graphics, vol. 34, no. 4, **(2010)**, pp. 409-423.
[27] M. Kim, A. Entezari, and J. Peters, "Box spline reconstruction on the face-centered cubic lattice", IEEE Transactions on Visualization and Computer Graphics, vol. 14, no. 6, **(2008)**, pp. 1523-1530.
[28] A. Entezari and T. Möller, "Extensions of the zwart-powell box spline for volumetric data reconstruction on the Cartesian lattice". IEEE Transactions on Visualization and Computer Graphics, vol. 12, no. 5, **(2006)**, pp. 1337-1344.
[29] M. Kim and J. Peters, "Fast and stable evaluation of box-splines via the beziér-form". Numerical Algorithms, vol. 50, no. 4, **(2009)**, pp. 381-399.

Authors

Guodong Wang, he received the B.S. degree in Computer Science from Northwestern Polytechnical University in 2000 and M.S. degree in Computer Science from China Aviction Academe in 2006. Now he is working in AVIC Computing Technique Research Institute, Xi'an. He is also a Ph.D. student in Computer Science at Northwestern Polytechnical University. His research interests include Machine Learning and Image Processing.

Jingbao Yang, he received the B.S. degree in Computer Science from Henan University in 2001, and he received the M.S. degree in China Aviction Academe, Xi'an in 2004. Now he is working in AVIC Computing Technique Research Institute, Xi'an. His research interests include Embedded Systems and Image Processing.

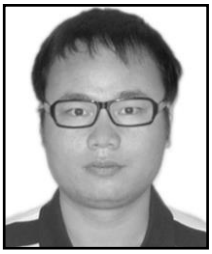

Yue Cheng, he received the B.S. degree and Ph.D. degree in Electronic Engineering from Zhejiang University in 2008 and 2013. Since 2013 he has been working in AVIC Computing Technique Research Institute, Xi'an. His research interests include Computer Vision and Image Processing.